

Epiartemisinin, a Remarkably Poor Antimalarial: Implications for the Mode of Action

by Charles W. Jefford*, Ulrich Burger, Patricia Millasson-Schmidt, and Gérald Bernardinelli

Department of Organic Chemistry and Laboratory of Crystallography, University of Geneva, CH-1211 Geneva 4

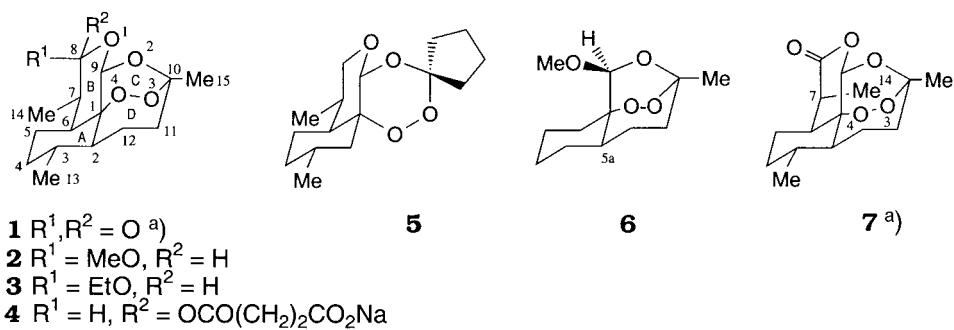
and Brian L. Robinson and Wallace Peters

Tropical Parasitic Diseases Unit, Northwick Park Institute for Medical Research, Harrow, Middlesex, HA1 3UJ, UK

Epiartemisinin (**7**) was prepared by the base epimerization of artemisinin (**1**) and its structure determined by X-ray analysis. The antimalarial activity of **7** against the chloroquine-sensitive and resistant strains of *Plasmodium berghei* and *P. yoelii* in the mouse was compared with that of the highly effective schizonticide **1** and found to be drastically diminished. It is argued that the mode of action on the intraerythrocytic parasite by **7** is compromised by steric hindrance arising from the α -disposed Me group. In the initial step, intimate complexation with heme is hindered or biased to favor the formation of a less potent C-centered radical, the final lethal agent.

1. Introduction. – The discovery that the tetracyclic 1,2,4-trioxane artemisinin (**1**), a constituent of the shrub *Artemisia annua*, is endowed with powerful antimalarial properties, has led to the development of semi-synthetic derivatives such as artemether, arteether, and artesunate (see **2–4**) [1] [2], and the wholly synthetic tricyclic analogues **5** and **6** [3]. Although somewhat expected, since the C-skeleton remains the same, it is nonetheless significant that the lactol derivatives **2–4**, regardless of the configuration at C(8), fully retain the activity of the parent structure. On the other hand, the high parasitocidal potency of **5** and **6** unambiguously demonstrates that rings B and D of **1** are superfluous, indicating that other residual structural features must be crucial for conferring high activity. We now describe how a minor alteration in the structure of artemisinin, namely, epimerization of the Me(14) substituent, brings about a dramatic diminution in antimalarial activity. Furthermore, it will be seen why the configuration at C(7) has a specific bearing on the mode of action.

Results and Discussion. – Treatment of **1** with 1,8-diazabicyclo[5.4.0]undec-7-ene (DBU) in a solution of MeCN at room temperature for 24 h brought about conversion to epiartemisinin (**7**) in 31% yield, the material remaining being artemisinin (**1**; 68%). Chromatography afforded a pure sample of **7**, which was characterized by its ¹H- and ¹³C-NMR spectra. Recrystallization gave a single crystal, thereby enabling its structure to be determined by X-ray analysis (*Fig. 1*). Apart from confirming the configuration at the C(7) position, important differences are discerned on comparing the structure of **7** with that of **1** [4]. Although the bond lengths and bond angles in both molecules are very nearly the same, the intra-annular torsional angles of the lactone ring reveal large divergences (*Table 1*). The result is that the lactone ring in **7** adopts an envelope



^{a)} The atom numbering of **1** and **7** is the same as that used for the crystal structure of **7** (see Fig. 1).

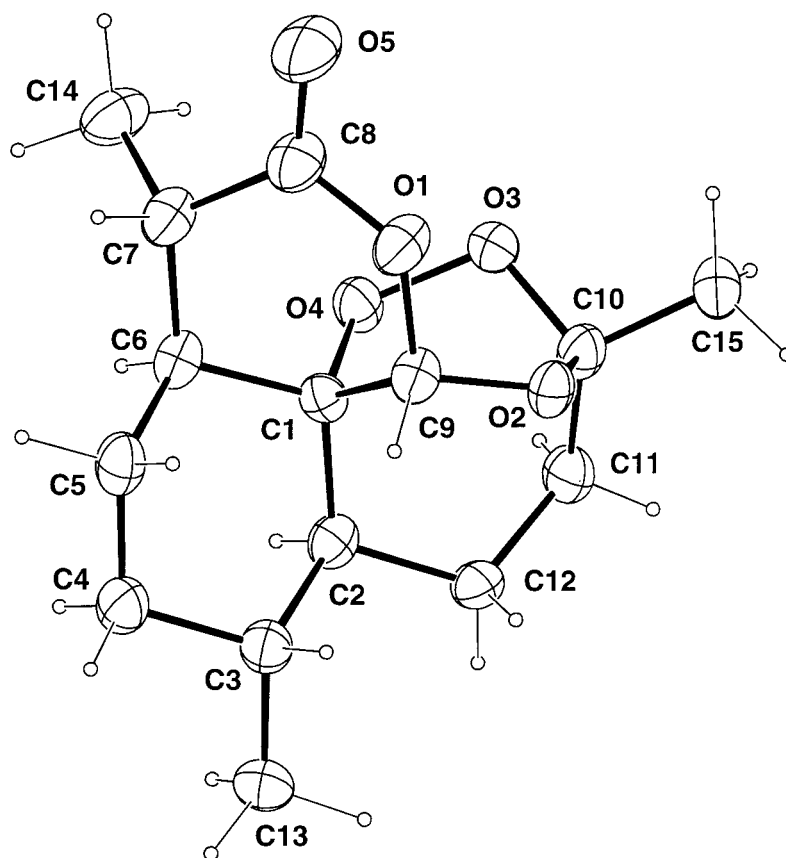


Fig. 1. Perspective view of the crystal structure of epiartemisinin (**7**). Arbitrary atom numbering. Ellipsoids are represented with 40% probability.

Table 1. *Intra-annular Torsional Angles* [°], *Minimum Values of Asymmetry Parameters* [6], and *Ring Conformations for Epiartemisinin (7) and Artemisinin (1)* [4]

	Epiartemisinin (7)	Artemisinin (1)
Cyclohexane C(6)–C(1)–C(2)–C(3)	– 52.2(5)	– 49.5
C(1)–C(2)–C(3)–C(4)	50.6(6)	46.1
C(2)–C(3)–C(4)–C(5)	– 53.1(6)	– 50.8
C(3)–C(4)–C(5)–C(6)	57.5(6)	56.9
C(4)–C(5)–C(6)–C(1)	– 57.7(6)	– 58.2
C(5)–C(6)–C(1)–C(2)	54.9(5)	55.5
Asymmetry parameter	$\Delta C_2(C(2)–C(3)) = 0.006$	$\Delta C_2(C(2)–C(3)) = 0.005$
Conformation	chair	chair
Lactone C(9)–C(1)–C(6)–C(7)	54.2(5)	59.0
C(1)–C(6)–C(7)–C(8)	– 25.9(6)	– 50.8
C(6)–C(7)–C(8)–O(1)	– 9.2(7)	28.4
C(7)–C(8)–O(1)–C(9)	15.8(7)	– 14.4
C(8)–O(1)–C(9)–C(1)	14.6(6)	22.7
O(1)–C(9)–C(1)–C(6)	– 49.0(5)	– 44.8
Asymmetry parameter	$\Delta C_s(C(1)) = 0.045$	$\Delta C_2(C(1)–C(6)) = 0.026$
Conformation	envelope	half-chair
1,2,4-Trioxane C(9)–C(1)–O(4)–O(3)	17.0(4)	12.2
C(1)–O(4)–O(3)–C(10)	45.2(4)	47.7
O(4)–O(3)–C(10)–O(2)	– 73.5(4)	– 75.5
O(3)–C(10)–O(2)–C(9)	32.8(5)	36.3
C(10)–O(2)–C(9)–C(1)	30.4(5)	24.7
O(2)–C(9)–C(1)–O(4)	– 56.8(5)	– 50.8
Asymmetry parameter	$\Delta C_2(C(1)–C(9)) = 0.046$	$\Delta C_2(C(1)–C(9)) = 0.044$
Conformation	twist-boat	twist-boat
Oxacycloheptane C(9)–C(1)–C(2)–C(12)	– 52.1(5)	– 51.8
C(1)–C(2)–C(12)–C(11)	– 35.8(6)	– 36.1
C(2)–C(12)–C(11)–C(10)	56.9(6)	56.3
C(12)–C(11)–C(10)–O(2)	23.6(6)	25.7
C(11)–C(10)–O(2)–C(9)	– 89.8(4)	– 87.2
C(10)–O(2)–C(9)–C(1)	– 95.2(4)	– 101.9
O(2)–C(9)–C(1)–C(2)	62.8(5)	67.2
Asymmetry parameter	$\Delta C_2(C(2)) = 0.032$	$\Delta C_2(C(2)) = 0.029$
Conformation [5]	twist-boat	twist-boat
Dioxacycloheptane C(2)–C(1)–O(4)–O(3)	– 105.5(4)	– 108.3
C(1)–O(4)–O(3)–C(10)	45.2(4)	47.7
O(4)–O(3)–C(10)–C(11)	47.2(4)	46.3
O(3)–C(10)–C(11)–C(12)	– 95.7(5)	– 94.2
C(10)–C(11)–C(12)–C(2)	56.9(6)	56.3
C(11)–C(12)–C(2)–C(1)	– 35.8(6)	– 36.1
C(12)–C(2)–C(1)–O(4)	68.7(5)	69.0
Asymmetry parameter	$\Delta C_2(O(3)) = 0.043$	$\Delta C_2(O(3)) = 0.048$
Conformation [5]	twist-chair	twist-chair

conformation, whereas in **1** it is a half-chair. It is important to note that the adjacent trioxane rings remain undisturbed; both are fixed in twist-boat conformations with a pseudo- C_2 axis passing through the C(1)–C(9) bond. Similarly, the oxacycloheptane rings in **7** and **1** exist as twist-boat conformations with a pseudo- C_2 axis passing through the O(3) atom. The cyclohexane and dioxacycloheptane rings [5] in each epimer take up chair and twist-chair conformations, respectively. It is also noteworthy that the asymmetry parameters [6] for each pair of rings, except for those of the lactone rings,

are remarkably consistent. In other words, the overall skeletons for **7** and **1**, especially the peroxide entities, are nearly superimposable except for the lactone rings and their critical Me(14) substituents.

Despite the flattening of the lactone ring in **7**, the Me(14) group lies uncomfortably close to the peroxide linkage. The interatomic distances between the C(14) atom and the O(3) and O(4) atoms are 4.068(6) and 3.216(6) Å, respectively. The latter distance is quite short and means that one of the H–C(14) atoms and O(4) are in *van der Waal's* contact.

The repercussions of the change of configuration at C(7) on the *in vivo* activity were next examined. Samples of **7** together with artemisinin (**1**) and chloroquine, by way of comparison, were tested against *Plasmodium berghei* N and *P. yoelii* ssp. NS in a rodent model [7]. The N strain is chloroquine-sensitive, whereas the NS strain is chloroquine-resistant. Samples were taken up in dimethyl sulfoxide (DMSO) and diluted serially with *Tween 80* in H₂O. Administration was by the subcutaneous (sc) route. The dose was administered daily to sets of infected mice for four days. On the fifth day, the parasitemia was determined. The effective doses, *ED*₅₀ and *ED*₉₀, namely for 50 and 90% suppression of parasites, respectively, when compared with untreated controls, were estimated from a plot of log dose/probit activity, and are expressed in mg/kg.

It is immediately seen that the α -epimer **7** is significantly less active than the naturally occurring β -epimer **1** (Table 2). Against the chloroquine-sensitive line, both the *ED*₅₀ and *ED*₉₀ values of **7** are about seven times greater than those of **1**. Similar loss of activity is observed against the resistant line. However, the loss is less marked for the *ED*₅₀ values, **7** being 4.3 times less active than **1**, but the difference between the *ED*₉₀ values is still sizable, being about six-fold. In all cases, **7** fares poorly when compared to chloroquine in both the sensitive and resistant lines. The net conclusion is that the α -epimer **7** is not without activity, but that it is simply some four to seven times less effective than its β -epimer (**1**¹). The reasons for this disparity undoubtedly hinge on the configuration at the C(7) position. Evidently, the Me(14) group, depending on its orientation, acts as a switch by varying the amount of parasitocidal action.

How the switch operates becomes understandable on looking at the mode of action. It is now reasonably certain from model experiments that artemisinin (**1**), its lactol

Table 2. *In vivo Antimalarial Activity*^{a)} of (+)-Artemisinin (**1**) and (+)-Epiartemisinin (**7**) against *P. berghei* N and *P. yoelii* ssp. NS

	<i>P. berghei</i> N		<i>P. yoelii</i> NS	
	<i>ED</i> ₅₀	<i>ED</i> ₉₀	<i>ED</i> ₅₀	<i>ED</i> ₉₀
1	2.0	3.5	5.8	10.0
7	14.0 (7.6–21.5)	23.0 (12.5–35)	25.0 (10.0–40.0)	57.0 (23.0–95.0)
Chloroquine	1.8	3.1	2.4	56

^{a)} Values, obtained by the sc route, are expressed as *ED* in mg/kg/day \times 4.

¹⁾ The fact that **7** is not totally inactive might also be attributed to partial equilibration to **1** under the physiological conditions in the mouse. If this were so, then the activity of **1** would be proportionately decreased by equilibration to **7**. In any event, **7** remains unaffected by exposure to H₂O and *Tween*.

derivatives **2–4**, and peroxidic antimalarials in general kill the malarial parasite in the blood of the host by a stepwise process of chemical induction [8–11]. During the trophozoite stage of the intraerythrocytic cycle, the parasites invade the red blood cells and digest the hemoglobin content to provide amino acids for nutrition. The discarded prosthetic group, heme, is soluble and toxic to the parasite. However, it is immediately disposed of by oxidation and polymerization to the insoluble malarial pigment, hemozoin. When the host is treated with an antimalarial peroxide, the aforementioned detoxification process is intercepted by coordination with heme. In the case of artemisinin (**1**), although the trioxane ring is locked in a boat conformation within a rigid tetracyclic skeleton, it adroitly maneuvers its O–O bond over the iron atom and forms an intimate complex **8** [8] [12] [13]. Inspection of a *Newman* projection of **1** reveals that the α -face is free of obstruction, the Me(14) group lying in an equatorial position away from the peroxide atoms (*Fig. 2*). Next, within the complex, a single electron is transferred from the 3d orbital of iron to the sigma antibonding orbital of the contiguous peroxide bond causing it to break (see *Scheme*). Breakage occurs to give two different oxy radicals **9** and **10**, which may or may not be in equilibrium with each other. In the former radical, the C(10)–C(11) bond undergoes spontaneous cleavage propelled by the formation of the thermodynamically stable acetate group, simultaneously creating the highly reactive ethyl radical **11**. In contrast, the oxy radical **10** simply rearranges by a 1,5 H-shift to the secondary C-centered radical **12**. Both radicals thereupon alkylate the protein (PP) of nearby parasites, causing their death. Lastly, protonation of the parasite-artemisinin-hemin adducts **13** and **14** so formed releases the alkylated proteins **15** and **16**, respectively, from their hemin attachments, which subsequently polymerize to hemozoin [14]. What happens overall is that a toxic C-centered radical replaces toxic heme²⁾.

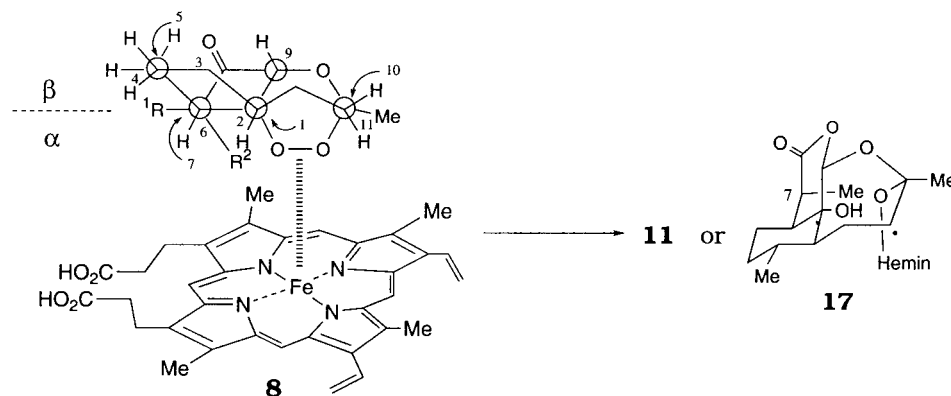
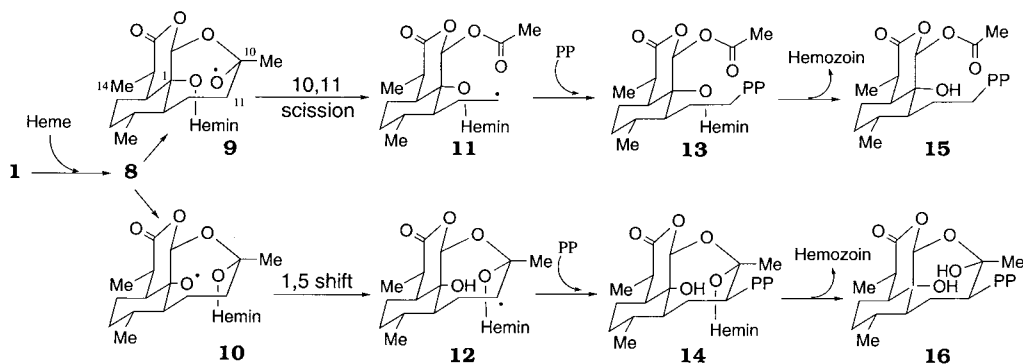


Fig. 2. Complex (**8**) formed between heme and the α -face of artemisinin (**1**; R¹ = Me, R² = H) or epiartemisinin (**7**; R¹ = H, R² = Me). The methyl substituent at C(3) is omitted for the sake of clarity. Arrows indicate numbering of eclipsed C-atoms. For **1**, the complex evolves mainly to **11**, whereas **7** favors **17**.

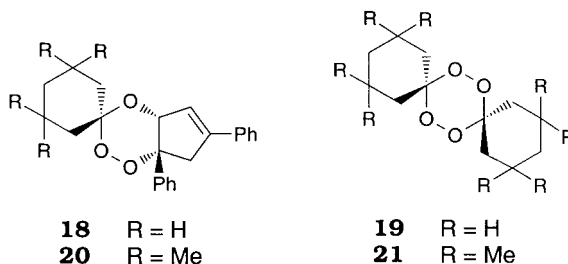
²⁾ To avoid any possible confusion about naming iron-containing porphyrins, we define hemin as having the same molecular structure as heme (see *Fig. 2*), except that it contains ferric ion bearing a positive charge [15]. Hemozoin is an irregular polymer of hemin joined by ferric carboxylate units [16].

Scheme



Ultimately, the parasiticidal power of artemisinin depends on the ease of formation of the primary and secondary radicals **11** and **12**, and, more importantly, on their proportions. Application of FeCl_2 to **1** as a mimic for heme has indicated that **11** is the dominant species [9c]. This is fortunate since **11** as a primary radical will alkylate more efficiently than **12**. It can now be appreciated why the epimer **7** is less potent as an antimalarial. The effect of the α -disposed Me(14) group is two-fold. First, it will hinder the closeness of docking with heme (Fig. 2). Second, it will skew complexation so that evolution to the corresponding less reactive, secondary radical **17** is favored.

The foregoing findings are entirely consonant with those observed for certain sterically encumbered 1,2,4-trioxanes and 1,2,4,5-tetroxanes that are markedly less active than their uncongested parents. For example, simply replacing H-C(5a) in trioxane **6** by a Me group gives a derivative devoid of *in vitro* activity [17]. A similar result is seen for the tetramethyl derivatives **20** and **21** of the cyclopenta-trioxane **18** and dispiro-tetroxane **19**, respectively [18]. The Me groups diminish activity by hindering complexation between heme and the peroxide bond. Alternatively, the C-centered radicals which might be formed from **20** and **21** would be poor alkylating agents owing to their intrinsic bulk at the β -position.



Conclusion. – The activity differences between artemisinin (**1**) and its C(7) epimer **7** are entirely consistent with a steric effect perturbing the cascade of chemically induced mechanistic events responsible for parasiticidal action. Optimally, the driving force for antimalarial activity derives from the thermodynamic stability acquired upon the simultaneous formation of the acetate group and the pendent ethyl radical, the lethal

agent. The epimer spoils this smooth course either by impeding docking or by switching rearrangement to the less reactive secondary C-centered radical. Modelling studies on epiartemisinin and tests with FeCl_2 as a diagnostic reagent are under way and will be reported later³⁾.

We are particularly grateful to *André Pinto* for help in determining the NMR spectra. Thanks are also due to Professor *F. Gulaçar* for the MS measurements.

Experimental Part

General. See [9c]. *Epimerization of Artemisinin 1.* A soln. of **1** (50 mg, 0.18 mmol) and 1,8-diazobicyclo[5.4.0]undec-7-ene (33 mg, 0.235 mmol) in dry MeCN (4 ml) under N_2 was stirred at r.t. for 24 h. Thereafter, the soln. was filtered over neutral alumina, which was subsequently rinsed with AcOEt and CH_2Cl_2 . The solvent was evaporated and the residue purified by flash chromatography [20] (neutral alumina, pentane/AcOEt, 9:1): **1** (33.9 mg, 68%) and **7** (15.5 mg, 31%). **7**: Colorless crystals. M.p. 158–160°. $[\alpha]_D^{25} = 71.59$ ($c = 0.95$, CHCl_3). IR (KBr): 2986–2834m, 1725s, 1452w, 1371m. $^1\text{H-NMR}$ (400 MHz, C_6D_6): 0.55 (*qd*, $J = 13.5$, 4.8 H–C(4)); 0.65 (*m*, Me(13), H–C(3)); 0.94 (*qd*, $J = 13.5$, 4.8 H–C(5)); 1.0–1.2 (*m*, H–C(2), H'–C(5), H'–C(4), H–C(12)); 1.23 (*dd*, $J = 13.5$, 5.0, H–C(6)); 1.31 (*s*, Me(15)); 1.48 (*m*, H'–C(12)); 1.57 (*d*, $J = 7.1$, Me(14)); 1.65 (*ddd*, $J = 13.4$, 5.4, 3.8, H–C(11)); 1.96 (*q*, $J = 7.4$, H–C(7)); 2.24 (*td*, $J = 13.4$, 5.4, H'–C(11)); 5.62 (*s*, H–C(9)). $^{13}\text{C-NMR}$ (100.6 MHz, C_6D_6): 19.8 (Me(13)); 20.8 (Me(14)); 25.0 ($\text{CH}_2(12)$); 25.5 (Me(15)); 30.7 ($\text{CH}_2(5)$); 34.0 ($\text{CH}_2(4)$); 36.1 ($\text{CH}_2(11)$); 37.1 (CH(3)); 40.1 (CH(7)); 45.5 (CH(7)); 50.4 (CH(2)); 80.5 (C(6)); 93.7 (CH(9)); 105.1 (C(10)); 171.1 (C(8)). EI-MS (70 eV): 282 (1; M^+ , $\text{C}_{15}\text{H}_{22}\text{O}_5^+$); 236 (4), 222 (12), 192 (42), 166 (20), 151 (36), 123 (32), 55 (100).

Crystal Structure of Epiartemisinin (7): $\text{C}_{15}\text{H}_{22}\text{O}_5$, M_r 282.3; $\mu = 0.817 \text{ mm}^{-1}$, $F(000) = 608$, $d_x = 1.329 \text{ g cm}^{-3}$; orthorhombic, $P2_12_12_1$, $Z = 4$; $a = 6.4443(8)$, $b = 9.445(2)$, $c = 23.182(5) \text{ \AA}$; $V = 1411.0(5) \text{ \AA}^3$; from 20 reflections ($35^\circ < 2\theta < 45^\circ$), colorless prism $0.11 \times 0.25 \times 0.40 \text{ mm}$ obtained by recrystallization from heptane/*i*-PrOH solution. Cell dimensions and intensities were measured at 200K on a *Stoe-STADI4* diffractometer with graphite-monochromated $\text{CuK}\alpha$ radiation (λ 1.5418 Å); ω - 2θ scans, scan width $1.05^\circ + 0.35 \text{ tg } \theta$, and scan speed $0.05^\circ/\text{s}$. $0 < h < 6$; $0 < k < 9$; $0 < l < 24$ and all antireflections of these; 2074 measured reflections, 1724 unique reflections of which 1538 were observable ($|F_o| > 4 \sigma(F_o)$); R_{int} for equivalent reflections 0.029. Data were corrected for Lorentz and polarization effects and for absorption [21] ($A_{\text{min,max}}^* = 1.094, 1.238$). The structure was solved by direct methods using MULTAN 87 [22], all other calculations used XTAL [23] system. Full-matrix least-squares refinement based on F using weight of $1/[\sigma^2(F_o) + 0.0001(F_o)^2]$ gave final values $R = 0.037$, $\omega R = 0.035$ for 248 variables and 1538 contributing reflections. The maximum shift/error on the last cycle was 0.0046. Non-methyl H-atoms were refined with a fixed value of isotropic displacement parameters ($U = 0.05 \text{ \AA}^2$). Methyl H-Atoms were refined with restraints on bond lengths and bond angles (free rotation). The final difference electron density map showed a maximum of +0.19 and a minimum of -0.17 \AA^{-3} .

Crystallographic data (excluding structure factors) have been deposited with the *Cambridge Crystallographic Data Centre* as deposition No. CCDC.140506. Copies of the data can be obtained free of charge on application to the CCDC, 12 Union Road, Cambridge CB2 1EZ, UK (fax: +44 (1223) 336-033; e-mail: deposit@ccdc.cam.ac.uk).

REFERENCES

- [1] C. C. Shen, L.-G. Zhuang, *Med. Res. Rev.* **1984**, *4*, 47; D. L. Klayman, *Science (Washington D.C.)* **1985**, *228*, 1049; A. R. Butler, Y.-L. Wu, *Chem. Soc. Rev.* **1992**, 85.
- [2] C. W. Jefford, in 'Advances in Drug Research', Eds. B. Testa and A. U. Meyer, Academic Press, New York, 1997, Vol. 29, p. 271.
- [3] C. W. Jefford, Y. Wang, G. Bernardinelli, *Helv. Chim. Acta* **1988**, *71*, 2042; C. W. Jefford, J. Velarde, G. Bernardinelli, *Tetrahedron Lett.* **1989**, *30*, 4485; C. W. Jefford, J. A. Velarde, G. Bernardinelli, D. H. Bray, D. C. Warhurst, W. K. Milhous, *Helv. Chim. Acta* **1993**, *76*, 2775.

³⁾ The applicability of FeCl_2 as a mimic of heme has been convincingly demonstrated by its action on arteflene [19].

- [4] I. Leban, L. Golic, M. Japelj, *Acta Pharm. Jugosl.* **1988**, 38, 71.
- [5] J. B. Hendrickson, *J. Am. Chem. Soc.* **1967**, 89, 7047.
- [6] M. Nardelli, *Acta Crystallogr. Sect. C* **1983**, 39, 1141.
- [7] W. Peters, J. H. Portus, B. L. Robinson, *Ann. Trop. Med. Parasit.* **1975**, 69, 155.
- [8] C. W. Jefford, D. Misra, J. C. Rossier, P. Kamalaprija, U. Burger, J. Mareda, G. Bernardinelli, W. Peters, B. L. Robinson, W. K. Milhous, F. Zhang, D. K. Gosser, S. R. Meshnick, in 'Perspectives in Medicinal Chemistry', Eds. B. Testa, E. Kyburz, W. Fuhrer, and R. Giger, Verlag Helvetica Chimica Acta, Basel, 1993, p. 459.
- [9] a) C. W. Jefford, S. Kohmoto, D. Jaggi, G. Timári, J.-C. Rossier, M. Rudaz, O. Barbuzzi, D. Gérard, U. Burger, P. Kamalaprija, J. Mareda, G. Bernardinelli, I. Manzanares, C. J. Canfield, S. L. Fleck, B. L. Robinson, W. Peters, *Helv. Chim. Acta* **1995**, 78, 647; b) C. W. Jefford, F. Favarger, M. G. H. Vicente, Y. Jacquier, *Helv. Chim. Acta* **1995**, 78, 452; c) C. W. Jefford, M. G. H. Vicente, Y. Jacquier, F. Favarger, J. Mareda, P. Millasson-Schmidt, G. Brunner, U. Burger, *Helv. Chim. Acta* **1996**, 79, 1475.
- [10] S. R. Meshnick, C. W. Jefford, G. H. Posner, M. A. Avery, W. Peters, *Parasitology Today* **1996**, 12, 79.
- [11] W.-M. Wu, Y. Wu, Y.-L. Wu, Z.-J. Yao, C.-M. Zhou, Y. Li, F. Shan, *J. Am. Chem. Soc.* **1998**, 120, 3316.
- [12] S. R. Meshnick, A. Thomas, A. Ranz, C. Xu, H. Pan, *Mol. Biochem. Parasitol.* **1991**, 49, 181.
- [13] K. L. Shukla, T. M. Gund, S. R. Meshnick, *J. Mol. Graph.* **1995**, 13, 215.
- [14] A. Dorn, R. Stoffel, H. Matile, A. Bubendorf, R. Ridley, *Nature (London)*, **1995**, 374, 269.
- [15] H. R. Mahler, E. H. Cordes, 'Biological Chemistry', 2nd edn., Harper and Row, New York, USA, 1966, p. 665.
- [16] A. F. G. Slater, A. Cerami, *Nature (London)* **1992**, 355, 167; A. F. G. Slater, W. J. Swiggard, B. R. Orton, W. D. Flitter, D. E. Goldberg, A. Cerami, G. B. Henderson, *Proc. Natl. Acad. Sci. U.S.A.* **1991**, 88, 325.
- [17] F. Zouhiri, D. Desmaële, J. D'Angelo, C. Riche, F. Gay, L. Cicéron, *Tetrahedron Lett.* **1998**, 39, 2969; F. Zouhiri, D. Desmaële, J. D'Angelo, J. Mahuteau, C. Riche, F. Gay, L. Cicéron, *Eur. J. Org. Chem.* **1998**, 2897.
- [18] C. W. Jefford, J.-C. Rossier, W. K. Milhous, *Heterocycles* **2000**, 52, 1345.
- [19] P. M. O'Neill, L. P. Bishop, N. L. Searle, J. L. Maggs, S. A. Ward, P. G. Bray, R. C. Storr, B. K. Park, *Tetrahedron Lett.* **1997**, 38, 4263.
- [20] W. C. Still, M. Kahn, A. Mitra, *J. Org. Chem.* **1978**, 43, 2923.
- [21] E. Blanc, D. Schwarzenbach, H. D. Flack, *J. Appl. Crystallogr.* **1991**, 24, 1035.
- [22] P. Main, S. J. Fiske, S. E. Hull, L. Lessinger, G. Germain, J.-P. Declercq, M. M. Woolfson, 'A System of Computer Programs for the Automatic Solution of Crystal Structures from X-Ray Diffraction Data', Universities of York, UK and Louvain-la-Neuve, Belgium, 1987.
- [23] XTAL 3.2 User's Manual, Eds. S. R. Hall, H. D. Flack, and J. M. Stewart, Universities of Western Australia, Australia, and Maryland, USA, 1992.

Received February 17, 2000